

Reconstructing the fast-ion velocity distribution in the DIII-D tokamak during Alfvén eigenmode activity

B. Madsen¹, M. Salewski¹, W. W. Heidbrink², L. Stagner², M. Podestà³, D. Lin²,
A. V. Garcia², P. C. Hansen⁴, J. Huang⁵ and the DIII-D team

¹ Department of Physics, Technical University of Denmark, Kgs. Lyngby, Denmark

² Department of Physics and Astronomy, University of California Irvine, Irvine, CA, USA

³ Princeton Plasma Physics Laboratory, Princeton, NJ, USA

⁴ Department of Applied Mathematics and Computer Science, Technical University of Denmark, Kgs. Lyngby, Denmark

⁵ Institute of Plasma Physics, Chinese Academy of Sciences, Hefei, Anhui, China

Abstract

Fast-ion velocity-space tomography enables reconstruction of the 2D fast-ion velocity distribution from a set of measurements. Here, we reconstruct the fast-ion velocity distribution for plasmas with strong and weak Alfvén eigenmode (AE) activity using the four-view fast-ion D-alpha (FIDA) diagnostics in the DIII-D tokamak. We find that the fast-ion losses due to strong AE activity are selective in velocity-space with a particularly strong density decrease in the population of co-going fast-ions with energies between 40 and 70 keV.

Introduction

Resonant interactions between fast ions and Alfvén eigenmodes (AEs) can lead to enhanced fast-ion transport [1, 2] that can potentially cause reduced heating efficiency and damage to the reactor walls. The fast-ion D-alpha (FIDA) diagnostics provides a way to map the fast-ion transport by measuring the radiation following Balmer-alpha transitions in neutralized fast deuterium ions [3]. The ions are neutralized by charge-exchange with beam neutrals, and the measurement volume is determined by the intersection between the FIDA line-of-sight and the neutral beam. From a set of FIDA measurements, the local fast-ion distribution can be reconstructed by fast-ion velocity-space tomography [4, 5, 6]. Here, we employ the four-view FIDA diagnostic to reconstruct the central fast-ion velocity distribution during weak and strong AE activity during the sequential discharges #153071 and #153072 in the DIII-D tokamak [2, 7, 8].

Velocity-space coverage of the DIII-D FIDA diagnostics

At a location in position space, the discrete FIDA spectrum S relates to the local fast-ion velocity distribution F through $S = WF$, where W is the transfer matrix containing the FIDA

weight functions [4, 9, 10] computed with FIDASIM [11]. Four distinct FIDA views looking onto three different neutral beams are installed in the DIII-D tokamak [2]. Fig. 1a-d show the modelled spectra for each view originating from an analytic fast-ion slowing down distribution (Fig. 2). The DIII-D FIDA diagnostics measures only one-sided spectra (unlike the FIDA systems at the ASDEX Upgrade [6], NSTX [12] and EAST [13] tokamaks), as indicated by grey-shaded areas in the figure. Fig. 1e shows how many FIDA views are sensitive to any given point in velocity space. Multiple-view coverage is required to obtain reliable reconstructions [14]. However, a large fraction of the negative-pitch velocity space is covered by only one view. Therefore, reliable reconstructions can be obtained for only positive pitches.

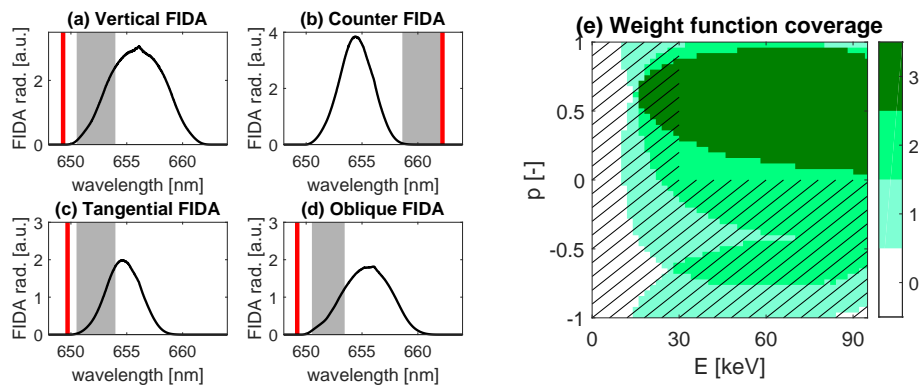


Figure 1: (a-d) Synthetic signals from an analytical co-going NBI slowing down distribution for each of the four FIDA views. The experimentally reliable wavelength ranges are marked in grey, whereas the red-shaded regions correspond to synthetic null-measurements [15]. (e) The number of views covering any given point in velocity space related to the grey-shaded areas in panels a-d. Here we trust only reconstructions in the area that is not scratched.

Reconstructions for positive pitches

In order to reconstruct the fast-ion distribution from measurements, the problem must be regularized [5]. This can be done by first-order Tikhonov regularization [16], where the solution is

$$F^* = \min_F \left\| \begin{pmatrix} W \\ \lambda_1 L_1 \end{pmatrix} F - \begin{pmatrix} S \\ 0 \end{pmatrix} \right\|_2. \quad (1)$$

Here L_1 approximates the gradient with respect to E and $p = v_{\parallel}/v$ [5], and λ_1 is the regularization strength. The solution is improved by including a non-negativity constraint [15] and null-measurements marked with red-shaded regions in Fig. 1a-d as a penalty [17]. Additionally, we introduce two new types of prior information for reconstructing for only positive pitches by assuming: (i) a known simulated signal originating from ions with negative pitches, and

(ii) isotropy for negative-pitch ions deposited in a one-dimensional energy-resolved bin. The resulting reconstructions from a noisy synthetic signal based on the analytical slowing-down distribution in Fig. 2a are shown in Fig. 2b-e. For all methods, the positive-pitch regions of the reconstructions are in good agreement with the ground truth.

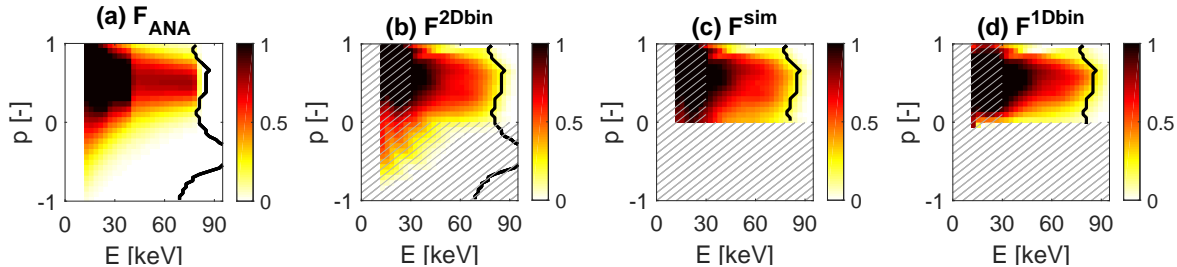


Figure 2: (a) Analytic fast-ion slowing down distribution from co-going neutral beam injection and (b-d) inversions of a synthetic signal from panel a. The superscripts indicate the employed inversion methods, and the normalization factors are the same.

The effect of AE activity on the positive-pitch fast-ion population

The DIII-D discharges #153071 and #153072 exhibit weak and strong AE activity, respectively [2, 7]. Due to calibration uncertainties, we only consider relative differences caused by increased mode activity. Fig. 3 shows the pitch spectra integrated over energies for $E > 30$ keV and energy spectra integrated over positive pitches for the pixel-differences between the central fast-ion velocity distributions during strong and weak AE activity. The spectra are computed both from the classically expected TRANSP/NUBEAM [18] distributions and reconstructions from measurements using the methods tested in Fig. 2. Compared to what is classically expected, the reconstructions observe a strong decrease in the local fast-ion density for energies between 40 and 70 keV and pitches greater than 0.2 caused by the increased AE activity.

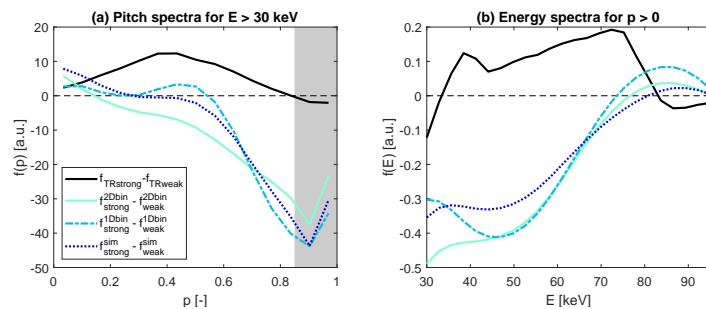


Figure 3: (a) Pitch spectra integrated over energy for $E > 30$ keV and (b) energy spectra integrated over pitch for $p > 0$ for the differences between the discharges with strong and weak AE activity from both the classical TRANSP/NUBEAM distributions and reconstructions.

Conclusion

The discharge with strong AE activity shows a strong decrease in the density of fast ions from the central plasma with pitches greater than 0.2 and energies between 40 and 70 keV compared to the discharge with weak AE activity. This is captured by all methods used to reconstruct the distribution from measurements, but not by the classical TRANSP/NUBEAM distributions, and is attributed to the increased AE activity.

Acknowledgments

We appreciate the support of the ITPA Topical Group for Energetic Particle Physics and the DIII-D team. This work has been carried out within the framework of the EUROfusion Consortium and has received funding from the Euratom research and training programme 2014-2018 and 2019-2020 under grant agreement No 633053. The views and opinions expressed herein do not necessarily reflect those of the European Commission. This material is based upon work supported by the U.S. Department of Energy, Office of Science, Office of Fusion Energy Sciences, using the DIII-D National Fusion Facility, a DOE Office of Science user facility, under Award DE-FC02-04ER54698, and by the U.S. Department of Energy, Office of Science, Office of Fusion Energy Sciences, Contract Number DE-AC02-09CH11466. DIII-D data shown in this paper can be obtained in digital format by following the links at https://fusion.gat.com/global/D3D_DMP.

References

- [1] W. W. Heidbrink *et al.*, Phys. Plasmas **15**, 055501 (2008)
- [2] W. W. Heidbrink *et al.*, Plasma Phys. Control. Fusion **56**, 095030 (2014)
- [3] W. W. Heidbrink *et al.*, Plasma Phys. Control. Fusion **46**, 1855 (2004)
- [4] M. Salewski *et al.*, Nucl. Fusion **52**, 103008 (2012)
- [5] A. Jacobsen *et al.*, Plasma Phys. Control. Fusion **58**, 045016 (2016)
- [6] M. Weiland *et al.*, Plasma Phys. Control. Fusion **58**, 025012 (2016)
- [7] C. T. Holcomb *et al.*, Phys. Plasmas **22**, 055904 (2015)
- [8] B. Madsen *et al.*, *Tomography of the positive-pitch fast-ion velocity distribution in DIII-D plasmas with Alfvén eigenmodes*, submitted
- [9] W. W. Heidbrink *et al.*, Plasma Phys. Control. Fusion **49**, 1457-1475 (2007)
- [10] M. Salewski *et al.*, Plasma Phys. Control. Fusion **56**, 105005 (2014)
- [11] L. Stagner *et al.*, *FIDASIM: A Neutral Beam and Fast-ion Diagnostic Modeling Suite*
- [12] M. Podestà *et al.*, Rev. Sci. Instrum. **79**, 10E521 (2008)
- [13] Y. M. Hou *et al.*, Rev. Sci. Instrum. **87**, 11E552 (2016)
- [14] M. Salewski *et al.*, Nucl. Fusion **58**, 096019 (2018)
- [15] M. Salewski *et al.*, Nucl. Fusion **56**, 106024 (2016)
- [16] P. C. Hansen, *Discrete Inverse Problems: Insight and Algorithms* (SIAM, 2010)
- [17] B. Madsen *et al.*, Rev. Sci. Instrum. **89**, 10D125 (2018)
- [18] A. Pankin *et al.*, Comput. Phys. Commun. **159**, 157 (2004)